

# Nonlinear growth dynamics of Langmuir monolayers limited by both surface and bulk diffusion

Alexandre Valance and Chaouqi Misbah

*Laboratoire de Spectrométrie Physique, Université Joseph Fourier (CNRS), Grenoble I, Boîte Postale 87, Saint-Martin d'Hères, 38402 Cedex, France*

(Received 2 December 1996)

A theory of growth of Langmuir monolayers limited by both surface and bulk impurity diffusion is developed. It is shown that unlike the traditional situation where only surface diffusion is present—leading to similarity solution where a straight front advances with time as  $\sqrt{t}$  which is at the basis of dendritic growth and “fractal-like” morphologies—bulk diffusion leads to the existence of a straight front moving at a constant speed. This is interpreted in terms of dimensional considerations: bulk diffusion introduces a new length scale, making this solution possible. As a consequence, the growth morphology must be dense. This is what is observed experimentally. An exact solution for a straight front and its stability is provided analytically. The straight front is unstable above a critical speed (or critical supersaturation). The nonlinear dynamics are tackled by means of a gauge-field-invariant geometrical formulation. It is shown that the existence of a straight front solution moving steadily also implies that a circular front solution moving at a constant speed exists as well. For a nearly straight geometry (but deformed) dynamics falls into a Kuramoto-Sivashinsky one where spatiotemporal chaos is expected. For a more curved front (such as the one generated initially from a circle instability), numerical analysis reveals a variety of compact patterns. [S1063-651X(97)08105-1]

PACS number(s): 47.20.Dr, 47.20.Hw, 81.10.Aj, 81.30.Fb

## I. INTRODUCTION

Langmuir-Blodgett films are important to studies of membrane structure and function, chemical reactions at an interface, and as coating for electronic and photonic devices. While the identification of Langmuir monolayers could be traced back at least to the last century [1], there has recently been an upsurge of interest in the study of structural and dynamical features of these systems [2–7]. These monolayers form at an air/water interface due to the amphiphilic nature of the molecules in question. Typical systems include fatty acids [8] such as pentadecanoic acid, or phospholipids [2] such as dimyristoylphosphatic acid (DMPA).

Besides their natural interest—these systems often represent the principal component of biological membranes—the physics of nonequilibrium patterns in these systems differs from that of more standard alloy solidification in two manners. First, these systems are unique truly two dimensional objects on the atomic scale. Hence the growth of domains between different phases is a problem of evolution of a one dimensional interface where we expect, for example, an enhanced role of statistical fluctuations. The second distinction lies in the ability to act easily on several parameters to which the growth structure may be quite sensitive. For example, the molecules may be quite susceptible to the *pH* modification. This results in interesting behaviors [10]. One can also devise a setup where the growth dynamics may be limited by added impurities which can either be miscible or not in water. In the latter case (impurities are not miscible in water) the growth pattern is strongly branched or occasionally dendritic. The seldom nature of dendrites may be a signature of the weakness of anisotropy of the growing crystal, may be related to the presence of a hexatic phase [9], or (more probably in our opinion) is due to the importance of noise (noise is expected to destroy the needle crystal when its magnitude is large enough) stemming from the one dimensional charac-

ter of the boundary, albeit crystalline anisotropy remains in a reasonable order of magnitude. The former case (impurities which are miscible in water) has recently been treated experimentally [11] and has constituted a source of stimulation for the present work. This experiment was performed on fatty alcohols where the impurities are fatty acids. The miscibility depends on the length of the fatty acid molecules. In this system, it has been observed that when impurities are miscible in water, then the branched structure disappears and rather compact (almost circular on some scale) morphologies are observed. It is one of the goals of this paper to show that this is attributed to bulk diffusion.

In the theory of traditional growth, one of the most important achievements in free crystal growth during the last decade is the resolution of the velocity (and tip radius) selection dilemma of a growing dendrite [13,14]. Usually when a solid alloy is grown at the expense of its undercooled melt, the predominant growth morphologies are dendritic (or completely faceted if the surface is below its roughening transition). Dendritic growth results because the front (which is a source of latent heat generation) has to heat a large bulk, since the temperature can nowhere exceed the freezing temperature. It is now well established that a planar front cannot grow at a constant speed. For such a geometry, the position increases as  $\sqrt{t}$  in the course of time. This is the so-called similarity solution, since the diffusion field does not depend separately on the spatial coordinate  $x$  and the temporal one  $t$ , but only on the combination  $x/\sqrt{t}$ . The absence of a planar front solution moving steadily can be traced back to a dimensional constraint: given the physical parameters that enter the problem, it is not possible to construct a quantity having the dimension of velocity.

It turns out that the similarity solution is unstable: the front undergoes a morphological instability. Since, as stated above, the front has to heat a large bulk, it has to curve as much as possible, so that far behind the advancing tip the

solid becomes asymptotically planar. We can use the feature of the similarity solution for the asymptotic solution in order to guess the famous parabolic solution in the absence of surface tension due to Ivantsov [15]. Thus from a simple analysis of similarity the equation relating the supersaturation to the Péclet number ( $p = \rho V/2D$ , where  $\rho$  is the radius of curvature,  $V$  the tip velocity, and  $D$  the diffusion constant) can be derived. Depending on the supersaturation and the strength of crystalline anisotropy, the pattern can be dendritic with a fractal character or a compact one, or having a rather branched (or seaweed) structure which can be fractal or compact as well [16]. We shall devote a brief review to the last decade of development.

The problem we are interested in has brought several new features. Here in contrast, due to diffusion in the bulk of water, there exists a planar front solution (more precisely a straight front solution since the growing front of our system is one dimensional) moving at a constant speed. This is attributed to the appearance of a length scale: the diffusion length of an impurity (which is rejected at the front, for example) before it enters the underlying bulk. This quantity is defined as  $\xi_s = \sqrt{D_s \tau}$ , where  $D_s$  is the diffusion constant and  $\tau$  the residence time on the surface. This quantity lies in the range of  $1 \mu\text{m}$ . From a dimensional analysis we argue that the front velocity is fixed by  $V \sim (\xi_s/\tau)\Delta$  where  $\Delta$  is an appropriate dimensionless supersaturation. The existence of bulk diffusion completely destroys the similarity solution. We have analyzed the stability of this solution and found that it becomes unstable above a critical supersaturation. The existence of a straight solution should have important consequences on the subsequent dynamics, and this is what will emanate from the present work. First, while the front becomes unstable, and even if it starts developing a needle, far behind the tip, the front should reach asymptotically a straight front solution moving at a constant speed given by  $v \cos(\theta) \sim (\xi_s/\tau)\Delta$ , where  $\theta$  is the angle between the growth axis and the normal (the opening angle), and  $v$  is the axial growth velocity. This implies that the front cannot be more curved beyond this limiting angle. Physically, diffusion in the bulk plays an efficient role of a short circuit, precluding thereby development of branched structures. We expect therefore the morphology to be compact as compared to the case where impurities are not miscible in water.

Above the straight front solution threshold, nonlinear effects come to the fore. Instead of using an integro-differential formulation of the free boundary problem, we shall make use of general concepts of symmetry, combined with a gauge-field-invariant formulation analogous to that developed for free dendritic growth [13]. We show by using only the concept of existence of a straight front solution moving steadily and the above mentioned formulation, that, for example, a circular solution moving at a constant speed exists as well. Then, by concentrating on a nearly curved front, we show that dynamics are described by a Kuramoto-Sivashinsky equation [17]. For a strongly curved front (for example, an initial circle that becomes unstable), we shall show, based on the invariant of the metrics, that the existence of the straight front solution leads to a completely different morphology than that found when a similarity solution was possible. We show, in particular, that the pattern in the presence of anisotropy is not reminiscent of those which arise in the case

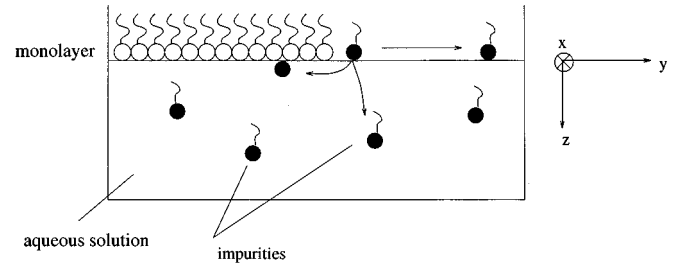


FIG. 1. A schematic view of the experimental setup.

where a similarity solution exists (which falls broadly in a dendritic or branched patterns).

The scheme of this paper is as follows. In Sec. II we present our model of growth of a condensed phase at the expense of its expanded phase, where the growth is limited by surface and bulk impurity diffusion. Section III is devoted to a qualitative analysis of the model together with a short survey of traditional growth. In Sec. IV, after arguing physically about the existence of a straight front solution, we study in detail this solution from the mathematical point of view. Section V deals with the linear stability analysis of the straight front solution. In Sec. VI we present the gauge-field-invariant formulation, and discuss its far reaching consequences. We then present the main outcome of the analysis. Section VII sums up the results.

## II. MODEL EQUATIONS

Let us consider a film of Langmuir monolayer growing on the water surface as schematically shown in Fig. 1. In reality the experimental device is different from traditional ones where growth is usually induced by applying a two dimensional pressure. An interesting alternative is to use the so-called ‘‘Gibbs’’ protocol [7] which consists of depositing a microscopic droplet of the amphiphilic system under consideration on the water surface. At ordinary temperatures there is a layer of ‘‘expanded’’ phase (EP) which spreads out on the water surface. The droplet thus serves as a reservoir whose chemical potential is fixed (while the number of particles inside fluctuates). Then, by lowering the temperature, the expanded phase undergoes a first order transition into the condensed one. We first consider a straight boundary where the condensed phase (CP) is advancing in the  $y$  direction. We shall assume that the growth is limited by impurity diffusion. We consider the general case where impurities are miscible in water, so that both diffusion on the surface and in the underlying water bulk are permissible. Let  $c_s(\rho, t)$  be the impurity concentration at the surface of water, and  $c_v(\mathbf{r}, t)$  their concentration in the bulk, where  $\rho = (x, y)$ , and  $\mathbf{r} = (x, y, z)$ . Since we shall be first interested in a straight front advancing in the  $y$  direction at a constant velocity  $V$  (which will ultimately be determined if such a solution is to exist), we find it convenient to write the transport equations in the rest frame. The surface and bulk concentrations then obey the following mass conservation equations. (i) *Bulk*,

$$D \nabla^2 c_v + V \frac{\partial c_v}{\partial y} = \frac{\partial c_v}{\partial t}, \quad (1)$$

where  $D$  is the bulk diffusion constant, and  $\nabla^2 = \partial^2/\partial x^2 + \partial^2/\partial y^2 + \partial^2/\partial z^2$  is the bulk Laplacian. (ii) *Surface*,

$$D_s \nabla_{\parallel}^2 c_s + V \frac{\partial c_s}{\partial y} + D \left( \frac{\partial c_v}{\partial z} \right)_{z=0} = \frac{\partial c_s}{\partial t}, \quad (2)$$

where  $D_s$  designates the surface diffusion constant, and  $\nabla_{\parallel}^2 = \partial^2/\partial x^2 + \partial^2/\partial y^2$  is the surface Laplacian. The last term on the left hand side of Eq. (2) stands for the exchange with the bulk, as will be clarified below. Indeed the quantity  $(\partial c_v/\partial z)_{z=0}$  is the mass flux across the water surface. This flux is composed of two contributions. There are impurities in the bulk characterized by a ‘‘diffusion’’ length  $\xi$ , or by a ‘‘drift’’ velocity  $D/\xi$  that will enter the surface from the underlying bulk. Similarly, impurities which are adsorbed on water are characterized by a diffusion length  $\xi_s$ , which is perhaps better represented by evoking their residence time  $\tau$ . The impurities leave the surface towards the bulk at a frequency  $1/\tau$ . At equilibrium mass balance implies that  $(D/\xi)c_v^{\text{eq}} = c_s^{\text{eq}}/\tau$  ( $\tau = \xi_s^2/D_s$ ). In an out-of-equilibrium situation there is a deviation from this equality, which must be counterbalanced by a flux across the surface. Therefore the bulk-to-surface mass exchange is described by the following kinetic relation:

$$\left( D \frac{\partial c_v}{\partial z} \right)_{z=0} = \frac{D c_v}{\xi} - \frac{c_s}{\tau}. \quad (3)$$

Before analyzing the order of magnitude of different parameters introduced above, we shall complete our description. At the front, whose instantaneous position is denoted by  $y = \zeta(x, t)$ , the jump of the normal derivative is related to the normal growth velocity by the continuity equation

$$v_n \Delta c = -D_s \left[ \left( \frac{\partial c_s}{\partial n} \right)_{y=\zeta^+} - \left( \frac{\partial c_s}{\partial n} \right)_{y=\zeta^-} \right], \quad (4)$$

where  $\Delta c$  is the miscibility gap (which will be taken constant), and  $v_n$  is the normal growth velocity. Here mass diffusion in the CP is neglected since the corresponding diffusion constant is several orders of magnitude smaller than that in the EP. Similarly, latent heat generation will not be accounted for given the fact that it diffuses much faster than the mass. Expression (4) must be understood as containing contributions from diffusion ahead and behind the advancing front as schematically represented in Fig. 1. In principle, an impurity which is rejected behind the front has a finite residence time on the CP/water interface before it diffuses possibly towards the bulk phase. In principle, one has to write an exchange mass balance between the CP/water surface (where molecules have the ability to be adsorbed) and the underlying water phase. This should amount to an equation similar to Eq. (3) with different kinetic coefficients. While this question can easily be incorporated in our description, we shall assume a symmetric model where the exchange between the adsorbed molecules and those in the bulk are identical for both  $y > \zeta$  and  $y < \zeta$ . Since the involved adsorption energy barriers are of the same order of magnitude on both sides, we do not expect this assumption to alter the main outcomes of

the present study. Therefore we have decided not to make the presentation too complex unnecessarily.

The above equations must be supplemented with kinetic equations at the front relating the lack of chemical equilibrium to the mass current across the front. For a molecularly rough front (a situation which is in principle expected to be always fulfilled for a one dimensional object), chemical equilibrium is instantaneously established. Expanding the chemical potentials on both sides of the front about a reference point, and using well known thermodynamical identities together with an ideal solution assumption [18], the equilibrium condition then implies a condition on the impurity concentration at the front

$$\frac{c_s(y=\zeta) - c_{s\infty}}{\Delta c} = \Delta - d_0 \kappa [1 + \beta \cos(4\theta)], \quad (5)$$

where we have introduced a dimensionless supersaturation  $\Delta = (T_M - mc_{s\infty} - T)/(m\Delta c) = (c_s^{\text{eq}} - c_{s\infty})/\Delta c$ .  $c_{s\infty}$  is the surface impurity concentration far ahead of the front,  $d_0 = \gamma T_M/(m\Delta c L a)$  is the so-called capillary length (where  $T_M$  is the melting temperature of the pure substance,  $m$  is the liquidus slope for the coexistence of the two dimensional CP and its melt,  $\gamma$  the line tension,  $L$  the latent heat of melting, and  $a$  the molecular length), and  $\kappa$  is the front curvature counted to be positive for a convex profile. The  $\theta$ -dependent prefactor in Eq. (5) accounts for line tension anisotropy, where  $\beta$  measures the strength of anisotropy, and  $\theta$  is the polar angle between the growth axis and the normal to the front. For definiteness we have chosen a fourfold symmetry. In the expression for the supersaturation  $\Delta$ ,  $T$  is the temperature of the system and  $c_s^{\text{eq}}$  is the surface concentration of impurities at the growing interface for a straight front.

Finally, the boundary condition far away in the bulk reads

$$c_v(z=d) = c_{v\infty}, \quad (6)$$

which corresponds to the initial impurity concentration in the bulk. Here  $d$  is the width of the diffusion layer in the bulk. The set of Eqs. (1)–(6) completely describes front dynamics. Before proceeding to the analysis, we shall first present a qualitative description.

### III. QUALITATIVE ANALYSIS AND SHORT REVIEW

According to Eq. (3), the surface-to-bulk current exchange is given by  $D c_v/\xi$ . From a dimensional analysis  $D/\xi$  is a frequency multiplied by an atomic distance. Of course at very large temperature the time needed for a molecule to enter the surface from the bulk is fixed by a molecular frequency. However, at ordinary temperatures, this is a thermally activated process, and there is a need to jump an energy barrier, which is nothing but the adsorption energy. Therefore

$$\frac{D}{\xi} \sim \nu a e^{-U_a/k_B T}, \quad (7)$$

where  $a$  is a molecular length,  $\nu$  a molecular frequency, and  $U_a$  is the adsorption barrier. Moreover, diffusion in the bulk implies a diffusion barrier  $U_d$ , so that  $D \sim \nu a^2 e^{-U_d/k_B T}$ . It follows that

$$\xi \sim a e^{(U_a - U_d)/k_B T}. \quad (8)$$

If the adsorption process is less favorable than the diffusion one (as we may expect), then  $U_a > U_d$ , and consequently  $\xi \gg a$ . That is to say, the length  $\xi$  is not a molecular ‘‘mean free path,’’ but may even reach values in the range of 1  $\mu\text{m}$  given the exponential dependence on energy scales. On the other hand, at equilibrium Eq. (3) yields

$$\frac{D\tau}{\xi} = \frac{c_s^{\text{eq}}}{c_v^{\text{eq}}}. \quad (9)$$

The quantity  $c_v^{\text{eq}}$  corresponds to the initial concentration for a given experiment, while  $c_s^{\text{eq}}$  is the equilibrium concentration of the adsorbed molecules. The bulk concentration is an experimental controlled quantity while the surface concentration can be estimated from neutron scattering [12]. The order of magnitude for the ratio can thus be extracted and hence an estimate for  $D\tau/\xi$ . Using experimental values of  $c_s^{\text{eq}}$  and  $c_v^{\text{eq}}$ , we find that  $D\tau/\xi \sim 0 \mu\text{m}$ .  $\sqrt{D_s\tau} = \xi_s$  ( $\sim \sqrt{D\tau}$  since  $D_s \sim D$ ) represents the diffusion length on the surface before the molecules have a chance to enter the bulk, which is of the same order as  $\xi$  for a situation where miscibility in water is sufficiently favorable. Then  $\xi \sim 0 \mu\text{m}$ . We shall keep in mind these orders of magnitude in the following.

Since the present paper is intended also for researchers from different disciplines than crystal growth, we have felt it worthwhile to provide a brief review of the last decade of developments in the study of interfacial pattern formation during free growth (as opposed to directional growth). In the absence of a bulk-to-surface exchange, the length scales discussed above ( $\xi$  and  $\xi_s$ ) are absent. This entails that (for a straight geometry) we are left with a problem which is free of an intrinsic length scale. The only parameters that enter the model are  $D$  and  $V$ . Therefore a straight front solution moving steadily at a velocity  $V$  cannot exist as a consequence of dimensional constraints. In order to fix a velocity we need to combine  $D$  to a length scale  $\ell$ , or a time scale  $\tau$ . Had such scales been available, then the velocity scale would have been fixed by  $D/\ell$  or  $\sqrt{D/\tau}$ . The only possibility to have a straight solution is that the velocity be not constant in time. Upon introduction of the time variable, a natural choice for velocity is  $\sqrt{D/t}$  (up to a dimensionless factor). This implies that the front position behaves as  $\sqrt{Dt}$ . This is nothing but the similarity solution to the diffusion equation (written in the laboratory frame)

$$D\nabla_{\parallel}^2 c = \frac{\partial c}{\partial t}, \quad (10)$$

which holds in the absence of surface-to-bulk exchange. Let  $Y = y/\sqrt{t}$  be a new variable, and assume that  $c(y,t) = c(Y)$  (the similarity assumption), then Eq. (10) becomes

$$D \frac{d^2 c}{dY^2} = -\frac{Y}{2} \frac{dc}{dY}, \quad (11)$$

the solution of which is easily found to be given by

$$c = \frac{c_{\text{eq}} - c_{\infty}}{\int_{y_0}^{\infty} e^{Y'^2/4D} dY'} \int_Y^{\infty} e^{-Y'^2/4D} dY' + c_{\infty}, \quad (12)$$

where we have imposed  $c(Y=\infty) = c_{\infty}$  and  $c(Y=y_0) = c_{\text{eq}}$ . The quantity  $y_0$  (undetermined for the moment) is defined in such a way that the instantaneous front position is given by  $y_i = y_0 \sqrt{t}$  (the subscript  $i$  refers to the interface). Since  $y_i/\sqrt{t} = Y_i$ , it follows that the front position in the similarity variable is given by  $Y_i = y_0$ . Hitherto, we did not evoke mass conservation at the front, which will result in a closure condition relating the supersaturation to the velocity amplitude  $y_0$  ( $y_0$  has in fact a dimension of  $\sqrt{D}$ ). Assuming for simplicity the one sided model, mass conservation at the front  $dy/dt = (D/\Delta c)(\partial c/\partial y)$  becomes  $y_0 = -(2D/\Delta c)(dc/dY)(Y=y_0)$ . Using expression (12), we obtain the sought relation

$$\Delta = \frac{\sqrt{\pi} y_0}{2\sqrt{D}} e^{y_0^2/(4D)} \text{erfc}[y_0/(2\sqrt{D})], \quad (13)$$

where  $\text{erfc}(x) = (2/\sqrt{\pi}) \int_x^{\infty} e^{-t^2} dt$  is the complementary error function.

In reality such a solution is unstable. Let us have a short digression. It is a bit puzzling at this juncture to note that usually one talks about the instability of a straight front [19] moving at a constant velocity, which is not only unstable, but which does not exist (except for  $\Delta = 1$ )—we may talk about a solution which is *structurally unstable*, in the sense that an arbitrarily small deviation from  $\Delta = 1$  completely destroys the existence of such a solution.

We expect in such a situation to have a dendritic growth. Dendrites take place because the front, which rejects impurities (or generates latent heat in a thermal model which is formally identical to the present one) has to undersaturate (or to heat in a thermal model) a large bulk of melt, since the concentration can nowhere exceed the equilibrium one (or the temperature can nowhere exceed the freezing temperature). Ivantsov [15] has indeed shown that the free surface tension problem admits a parabolic solution moving steadily. This solution can also be understood from the above similarity solution. Indeed, if the front has to undersaturate a large bulk, it has to curve in such a way that far behind the tip of the advancing solid, the front becomes more and more straight (see Fig. 2). There the coordinate  $x$  must reach asymptotically the solution  $x = x_0 \sqrt{t}$  according to the above similarity solution. If a needle has to move at a constant speed  $y = v_0 t$ , the only way to have a shape-preserving solution is to impose  $y \sim x^2$ , which is a parabola. Setting  $y = -x^2/(2\rho)$  (where  $\rho$  is the parabola radius of curvature), we immediately identify that  $x_0 = \sqrt{2\rho v_0}$ . Using in relation (13) the quantity  $x_0$  instead of  $y_0$  we get immediately the famous Ivantsov relation which is usually obtained after several, more or less tedious, mathematical manipulations [15,20],

$$\Delta = \sqrt{\pi p} e^p \text{erfc}(\sqrt{p}), \quad (14)$$

where  $\Delta = (c_{\text{eq}} - c_{\infty})/\Delta c$  is the dimensionless supersaturation,  $p = \rho v_0/(2D)$  is the Péclet number. It can easily be checked that relation (14) holds for  $\Delta < 1$ . In the limit where  $\Delta \rightarrow 1$ ,  $\rho \rightarrow \infty$ , which corresponds to the limit of a straight

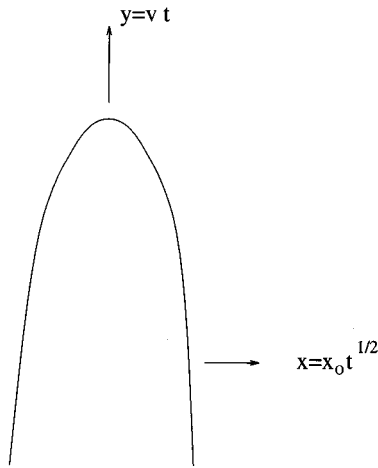


FIG. 2. A parabolic solution showing the use of similarity solution.

front. Relation (14) shows that there exists a continuous family of solutions for the couple  $(\rho, v_0)$ , whereas experiments show that a unique solution is selected for a given  $\Delta$ . This is the Ivantsov dilemma which has given rise to a myriad of studies in the 1980s [13,14]. The Ivantsov dilemma follows again from dimensional considerations. Indeed, in the absence of surface tension (or more precisely line tension in our problem), the capillary length introduced in Eq. (5) does not enter the problem, and again the same dimensional analysis evoked above for a straight front holds. In order to remove this degeneracy, we need to introduce surface tension which leads to the appearance of a new length scale  $d_0$ . A dimensional requirement is necessary but may not be sufficient. This is what happens precisely in the present problem. The Ivantsov dilemma has in fact been resolved only after the recognition (i) that surface tension acts as a singular perturbation and (ii) that crystalline anisotropy is necessary in order to lead to dendrites. In the absence of crystalline anisotropy [which enters in a natural way in line tension; see Eq. (5)], a needle crystal can initially grow. However, in the course of time the needle suffers from successive tip-splitting instabilities leading ultimately to a branched morphology. Anisotropy stabilizes the tip; it leads to a stable pattern having features similar to those which arise during snowflake growth. As displayed in Fig. 3, a dendrite generates sidebranches as it moves. The conventional wisdom is that sidebranches result from noise amplification. Indeed, a small perturbation on the tip (say, of thermal origin), is exponentially amplified as it moves downwards. While an initial perturbation is initially small (presumably of the molecular size, due to the very nature of thermal noise), a protuberance of appreciable amplitude may have grown at some distance from the tip. For example, in numerical solutions, the numerical noise is sufficient to produce sidebranches. Sidebranch activity is recognized as being “dangerous” against tip stability. More precisely, the noise amplification is stronger and stronger (and therefore the point where amplification has attained an appreciable amplitude is closer and closer to the tip) when anisotropy becomes gradually weaker. We expect a destruction of needle crystal solutions, and the emergence of branched structures. Whether a branched solution may become fractal or not was addressed in an interesting paper by

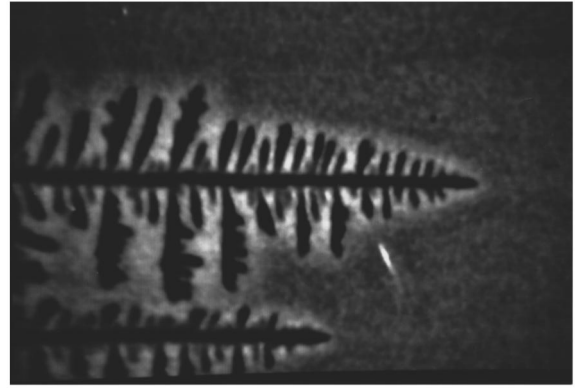


FIG. 3. Dendrite grown in a Langmuir monolayer of D-myristol alanine, as observed by epifluorescence microscopy. The bright halo around the dendrite corresponds to the diffusion layer of the fluorescent dye (insoluble in water) in the EP.

Uwaha and Saito [21], who have provided a beautiful interpolation between the fractal pattern (which is expected for a vanishing supersaturation) and a dense one (or what is usually called the Eden morphology) which should be attained on increasing the supersaturation. More recently Brener, Müller-Krumbhaar, and Temkin [16], using Uwaha and Saito’s results, along with previous analyses, have provided a nice phase diagram in the plane (supersaturation  $\Delta$ , the strength of crystalline anisotropy  $\beta$ ). They distinguish between dense and fractal patterns. Very schematically (i) for low  $\Delta$  and  $\beta$  we expect “fractal” patterns. For low  $\beta$  we expect ordinary fractals, while on increasing  $\beta$  “fractal dendrites” should appear (the structure is fractal, but it still keeps the memory of an underlying snowflakelike pattern). (ii) Large  $\beta$  and large  $\Delta$ : here the pattern is dense (or compact). For small  $\beta$  the dendrite identity is lost, and the resulting pattern is called compact seaweed. On increasing  $\beta$ , dendritic patterns which are compact are expected.

#### IV. GROWTH IN THE PRESENCE OF BULK-TO-SURFACE EXCHANGE: STRAIGHT FRONT SOLUTION

As discussed above, allowing for bulk-to-surface exchange provides us with several length scales  $\xi$  and  $\xi_s$ . Before resorting to a systematic analysis we shall first focus on the qualitative aspect. The impurities which are rejected at the front will diffuse on the surface, and their residence time is given by  $\tau$ . Their diffusion length is  $\xi_s = \sqrt{D_s \tau}$ . If this length is infinite, then we expect no exchange between surface and bulk. We are back to the traditional situation. The length must be finite. Thus  $\xi_s$  appears as a relevant length scale. From a dimensional analysis the scale of the growth velocity is given by  $D/\xi_s$ . The growth velocity is proportional to the driving force, so that

$$V \sim \frac{D_s}{\xi_s} \Delta. \quad (15)$$

Typically  $D_s \sim 10^{-6}$  cm<sup>2</sup>/s and  $\xi_s \sim 10^{-4}$  cm, so that  $V \sim 10^{-2} \Delta$  cm/s. The lack of information on the phase diagram of the amphiphilic system precludes a precise evaluation of the dimensionless supersaturation. Usually, in ordinary experiments, a small supersaturation  $\Delta \sim 0.1$  or even

0.01 is largely sufficient to initiate the growth. This amounts to  $V$  in the range of  $1 \mu\text{m/s}$ , which is consistent with experimental observations [11].

Let us now proceed to the calculation. Our starting point is the set of Eqs. (1) and (2), where we look for a straight front solution moving at a constant speed  $V$ . We find it convenient to set  $u = c_s(y) - (\tau D/\xi)c_v|_{z=0}$  and  $w = c_v(y, z) - c_{v\infty}$ . Equations (1)–(3) become

$$D \left( \frac{\partial^2 w}{\partial y^2} + \frac{\partial^2 w}{\partial z^2} \right) + V \frac{\partial w}{\partial y} = 0, \quad (16)$$

$$D_s \left( \frac{\partial^2 u}{\partial y^2} + \frac{\xi_s^2}{\xi} \frac{\partial^2 w}{\partial y^2} \Big|_{z=0} \right) - \frac{u}{\tau} + V \left( \frac{\partial u}{\partial y} + \frac{\xi_s^2}{\xi} \frac{\partial w}{\partial y} \Big|_{z=0} \right) = 0, \quad (17)$$

$$D \frac{\partial w}{\partial y} \Big|_{z=0} = -\frac{u}{\tau}. \quad (18)$$

Use of Fourier transforms with respect to the  $y$  coordinate leads to algebraic equations relating  $\hat{w}$  and  $\hat{u}$  (where  $\hat{w}$  and  $\hat{u}$  are Fourier transforms of  $w$  and  $u$ , respectively). Care should be taken, however. Indeed,  $\partial u/\partial y$  is discontinuous at  $y=0$ . Therefore when integrating by parts we should retain

the contribution of the  $\delta$  function. The remaining parts of the operations are straightforward. Using the fact that  $\hat{w}(q, z=d)=0$  [which follows from Eq. (6), and where  $q$  designates the variable in Fourier space] we can express  $\hat{w}$  as a function of  $\hat{u}$ . The result is

$$\hat{w} = -\frac{\hat{u}(q)}{\xi_s^2 r} \frac{\sinh r(z-d)}{\cosh(rd)}, \quad (19)$$

where

$$r_{\pm} = \frac{1}{\sqrt{2}} [\sqrt{q^4 + V^2 q^2 D^{-2} + q^2}]^{1/2} \pm \frac{1}{\sqrt{2}} [\sqrt{q^4 + V^2 q^2 D^{-2} - q^2}]^{1/2}, \quad (20)$$

where the  $+$  and  $-$  branches are adopted for  $q < 0$  and  $q > 0$ , respectively, to ensure well behaved solutions. Using the surface equation (17) where the discontinuity of  $\partial u/\partial y$  at the front (such a discontinuity is related to the growth velocity) arises after integration by parts, together with Eq. (19), and exploiting the fact that the normal velocity (4) is related to the jump of  $\partial u/\partial y$ , we obtain

$$\hat{u} = \frac{V\Delta c}{D_s} \frac{1}{[q^2 + \xi_s^{-2} + q^2(\xi r)^{-1} \tanh(rd)] - iqVD_s^{-1}[1 + (\xi r)^{-1} \tanh(rd)]}. \quad (21)$$

In real space the concentration fields can be represented by Fourier integrals

$$u(y) = \frac{V\Delta c}{2\pi D_s} \int_{-\infty}^{\infty} dq \frac{e^{-iqy}}{[q^2 + \xi_s^{-2} + q^2(\xi r)^{-1} \tanh(rd)] - iqVD_s^{-1}[1 + (\xi r)^{-1} \tanh(rd)]}, \quad (22)$$

$$w(y, z) = \frac{V\Delta c}{2\pi D_s \xi_s^2} \int_{-\infty}^{\infty} dq \frac{\sinh r(z-d)}{r \cosh(rd)} \frac{e^{-iqy}}{[q^2 + \xi_s^{-2} + q^2(\xi r)^{-1} \tanh(rd)] - iqVD_s^{-1}[1 + (\xi r)^{-1} \tanh(rd)]}. \quad (23)$$

Finally the growth velocity as a function of the supersaturation is determined by making use of the condition on  $c_s(y)$  at  $y=0$  [Eq. (5)] which takes the following form in the new representation:

$$c_s^{\text{eq}} - c_{s\infty} = u|_{y=0} + \xi_s^2 \xi^{-1} w|_{y=0, z=0}. \quad (24)$$

In view of Eqs. (22) and (23) the growth velocity should fulfill the equation

$$\Delta = \frac{V}{2\pi D_s} \int_{-\infty}^{\infty} dq \frac{1 + (r\xi)^{-1} \tanh(rd)}{[q^2 + \xi_s^{-2} + q^2(\xi r)^{-1} \tanh(rd)] - iqVD_s^{-1}[1 + (\xi r)^{-1} \tanh(rd)]}. \quad (25)$$

We recall that  $\Delta = (c_s^{\text{eq}} - c_{s\infty})/\Delta c$  represents the dimensionless supersaturation. Equation (25) relates  $V$  to the driving force  $\Delta$ . Note that this is a nonlinear equation since the quantity  $r$  which appears in the integrand is parametrized by the velocity [see Eq. (20)]. The integral can easily be tabulated, and  $V$  as a function of  $\Delta$  can then be extracted. Let us first focus on a limiting case where further analytical results can be obtained. This is encountered when the impurities reach their bulk value ( $c_{v\infty}$ ) on short scale as compared to all the

other lengths. This limit corresponds to  $d/\min(\xi, \xi_s) \ll 1$ . In this case the integral in Eq. (25) reduces to the evaluation of

$$\lim_{(y \rightarrow 0)} \int_{-\infty}^{\infty} dq \frac{e^{-iqy}}{q^2 + \xi_s^{-2} - iqVD_s^{-1}} = \frac{2D_s \pi}{V \sqrt{1 + 4D_s^2/(V^2 \xi_s^2)}}. \quad (26)$$

It then follows from Eq. (25) that  $V$  is given by

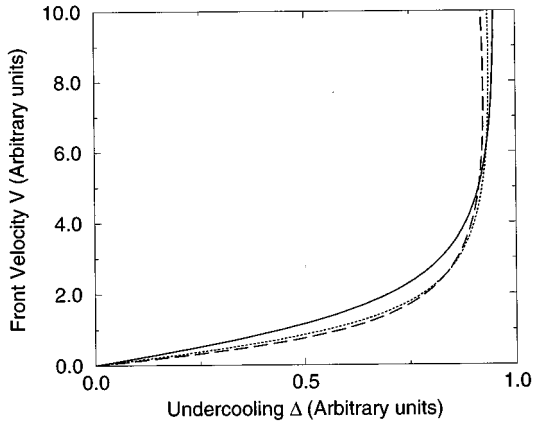


FIG. 4. The behavior of  $V$  as a function of  $\Delta$ . Full line: analytic theory [Eq. (27)]. Dotted line:  $d = \xi = \xi_s = 1 \mu\text{m}$ . Dashed line:  $\xi = \xi_s = 1 \mu\text{m}$ , and  $d = 2 \mu\text{m}$ .

$$V = 2 \frac{D_s}{\xi_s} \frac{\Delta}{\sqrt{1 - \Delta^2}}. \quad (27)$$

Equation (27) is what was anticipated from a dimensional analysis for a small supersaturation. That  $V$  seems to diverge for  $\Delta \rightarrow 1$  is not a surprise. This simply means that the liquid is supersaturated at the solidus line, and that therefore the solid should grow instantaneously. Of course before that regime is reached, our assumption of instantaneous chemical equilibrium at the front breaks down. Kinetics are expected to be relevant when the diffusion time  $D/V^2$  becomes comparable to the freezing time  $l/V$  where  $l$  is the CP-EP transition extent. Typically  $l$  is a molecular length ( $l \sim 10^{-8}$  cm at most),  $D \sim 10^{-6}$  cm<sup>2</sup>/s, so that the order of magnitude of the growth velocity where kinetics become decisive is given by  $V \sim D/l \sim 10^2$  cm/s, which is several orders of magnitude larger than what we are interested in. This corresponds to a supersaturation of the order  $\Delta \sim 1/(1 + l^2/\xi_s^2)^{1/2} \sim 1$ . Both Eqs. (27) and (25) are understood to be valid for  $\Delta$  not too close to unity.

Figure 4 shows  $V$  as a function of  $\Delta$  for several values of the parameters  $\xi$ ,  $\xi_s$ , and  $d$ , and comparison with expression (27) is made. It is clear that the latter captures the essential qualitative features. In conclusion of this section we have shown that diffusion in the bulk leads to the existence of a straight front solution moving at a constant velocity. It can also be shown that the similarity solution (viewed as an asymptotic solution) is destroyed by bulk diffusion [22]. The natural next step is to study the linear stability.

## V. LINEAR STABILITY ANALYSIS

We study regression of fluctuations by looking for solutions of the form

$$u(x, y) = u_0(y) + \epsilon u_1(y, z) e^{ikx + \omega t}, \quad (28)$$

$$w(x, y, z) = w_0(y, z) + \epsilon w_1(y, z) e^{ikx + \omega t}, \quad (29)$$

The subscript zero refers to the straight front solution, and  $\epsilon$  is a small parameter. The instantaneous front position is written as

$$\zeta(x, t) = \epsilon \zeta_1 e^{ikx + \omega t}, \quad (30)$$

where  $\zeta_1$  is a constant amplitude. Note that because Fourier modes do not couple in the linear regime, it suffices to consider one Fourier component only. In Eqs. (28) and (29)  $k$  is the perturbation wave number and  $\omega$  is the amplification or attenuation rate that we wish to determine. The transport equations read

$$-k^2 w_1 + \nabla_{\parallel} w_1 = 0, \quad (31)$$

$$D_s \left( -k^2 u_1 + \frac{\partial^2 u_1}{\partial y^2} - \frac{\xi_s^2}{\xi} k^2 w_1 \Big|_{z=0} + \frac{\xi_s^2}{\xi} \frac{\partial^2 w_1}{\partial y^2} \Big|_{z=0} \right) - \frac{u_1}{\tau} = 0. \quad (32)$$

The kinetic equation takes the form

$$D \frac{\partial w_1}{\partial z} \Big|_{z=0} = -\frac{u_1}{\tau}. \quad (33)$$

It must be noted that the boundary conditions at the front are to be evaluated at  $z = \zeta$ , and that therefore the zeroth order solutions are nonlinear functions of  $\epsilon$ , and they will contribute to the first order in  $\epsilon$  as well. For example, Eq. (4) becomes to first order in  $\epsilon$

$$\omega \zeta_1 \Delta c = -D_s \left[ \left( \frac{\partial u_1}{\partial y} + \zeta_1 \frac{\partial^2 u_0}{\partial y^2} \right) \Big|_{y=0+} - \left( \frac{\partial u_1}{\partial y} + \zeta_1 \frac{\partial^2 u_0}{\partial y^2} \right) \Big|_{y=0-} \right], \quad (34)$$

while the condition at the front on  $c_s$  [see Eq. (5)] leads to

$$\Delta c k^2 d_0 \zeta_1 = u_1|_{y=0} + \zeta_1 \frac{\partial u_0}{\partial y} \Big|_{y=0} + \frac{\xi_s^2}{\xi} \left( w_1|_{y=0, z=0} + \zeta_1 \frac{\partial w_1}{\partial y} \Big|_{y=0, z=0} \right). \quad (35)$$

Finally the boundary condition far in the bulk amounts to

$$w_1(z = d) = 0. \quad (36)$$

The set of Eqs. (28)–(36) constitutes the linearized version of front dynamics. Using the same procedure as in the zeroth order case, we can express the deviation  $u_1$  and  $w_1$  in terms of Fourier integrals. We shall give directly the results

$$u_1(y) = \frac{\xi_1}{2\pi} \left( \frac{\omega \Delta c}{D_s} + 2 \frac{\partial^2 u_0}{\partial y^2} \Big|_{y=0} \right) \int_{-\infty}^{\infty} dq \frac{e^{-iqy}}{[k^2 + q^2 + \xi_s^{-2} + \xi^{-1} \sqrt{k^2 + q^2} \tanh(d \sqrt{k^2 + q^2})]}, \quad (37)$$

$$w_1(y, z) = - \frac{\xi_1}{2\pi \xi_s^2} \left( \frac{\omega \Delta c}{D_s} + 2 \frac{\partial^2 u_0}{\partial y^2} \Big|_{y=0} \right) \times \int_{-\infty}^{\infty} dq \frac{\sinh \sqrt{k^2 + q^2} (z-d)}{\sqrt{k^2 + q^2} \cosh(\sqrt{k^2 + q^2} d)} \frac{e^{-iqy}}{[k^2 + q^2 + \xi_s^{-2} + \xi^{-1} \sqrt{k^2 + q^2} \tanh(\sqrt{k^2 + q^2} d)]}. \quad (38)$$

The dispersion relation is obtained by making use of Eq. (36). This yields

$$\left( \frac{\omega \Delta c}{D_s} + 2 \frac{\partial^2 u_0}{\partial y^2} \Big|_{y=0} \right) \int_{-\infty}^{\infty} \frac{dq}{2\pi} \frac{1 + (\xi \sqrt{k^2 + q^2})^{-1} \tanh(\sqrt{k^2 + q^2} d)}{[k^2 + q^2 + \xi_s^{-2} + \xi^{-1} \sqrt{k^2 + q^2} \tanh(\sqrt{k^2 + q^2} d)]} = - \Delta c d_0 k^2 - \left( \frac{\partial u_0}{\partial y} + \xi_s^2 \xi^{-1} \frac{\partial w_0}{\partial y} \Big|_{y=0, z=0} \right). \quad (39)$$

This is the sought dispersion relation which relates the growth rate  $\omega$  to the wave number  $k$ . As for the straight front solution, the integrals over  $q$  can be tabulated. It is instructive, however, to focus on the situation where  $d$  is small since a complete analytical evaluation of the integrals becomes possible. In this limit  $u_0$  and  $w_0$  are easily found to be given by

$$u_0(y) = \frac{\Delta c V \xi_s}{2D_s} e^{-|y|/\xi_s}, \quad (40)$$

$$w_0(y, z=0) = 0. \quad (41)$$

The last equation simply states that the bulk concentration is homogeneous; it simply serves as a reservoir for impurities. It is straightforward to show that Eq. (39) reduces to

$$\omega = 2D_s [-d_0 k^2 \sqrt{k^2 + \xi_s^{-2}} + \xi_s^{-1} \Delta (\sqrt{k^2 + \xi_s^{-2}} - \xi_s^{-1})]. \quad (42)$$

$\omega$  has two contributions: the first one is proportional to  $d_0$  (which is proportional to the line tension) and it is stabilizing. The second one is destabilizing and is proportional to the driving force  $\Delta$ . This expresses the enhancement of the diffusion gradient ahead of the front due to a protuberance. Thus the stability of the straight geometry results from a compromise between these two antagonistic effects. Further analytical results follow. A close inspection of Eq. (42) shows that the bifurcation from the straight geometry into a corrugated one occurs for  $k \rightarrow 0$  (actually this result holds in general and can be traced back to translational symmetry in the  $y$  direction). In the small  $k$  regime Eq. (42) reads to leading order

$$w \approx \frac{2D_s d_0}{\xi_s} [(\nu - 1)k^2 - (\nu + 1)\xi_s^2 k^4 / 2], \quad (43)$$

where  $\nu = \Delta \xi_s / (2d_0)$ . The straight front is unstable if  $\nu > 1$  and stable for  $\nu < 1$ . The critical condition occurs for  $\nu = 1$ . Figure 5 shows  $\omega$  as a function of  $k$  (which conserves the same qualitative feature in the general case) above and below the instability threshold. The fastest growing mode (obtained

by setting  $\partial\omega/\partial k = 0$ ) corresponds to a wave number  $k_{\max}$  and a growth rate  $\omega_{\max}$  given by

$$k_{\max} = \xi_s^{-1} \sqrt{\frac{\nu-1}{\nu+1}}, \quad \omega_{\max} = \frac{D_s d_0 (\nu-1)^2}{\xi_s^3 (\nu+1)}. \quad (44)$$

The  $\nu$ -dependent prefactors are of order unity above the threshold. This means that the length scale of the pattern corrugation is roughly of the order of  $\xi_s$ , and the temporal scale for the evolution of the instability is of the order of  $\xi_s^3 / (d_0 D_s) \sim (\xi_s / d_0) \tau$ . Since we expect that  $\xi / d_0 \sim 10^2 - 10^3$ , the time scale for the evolution of the instability should give a direct access to the estimate of  $\tau$ . In the experiment of Lenne *et al.* [11], the time scale for the instability is of the order of 1 sec (or a few seconds). This entails that  $\tau$  can roughly be estimated to lie in the range  $10^{-1} - 10^{-2}$  s.

## VI. NONLINEAR REGIME

The linear stability analysis provides us with the critical condition for the onset of the instability, and the range of

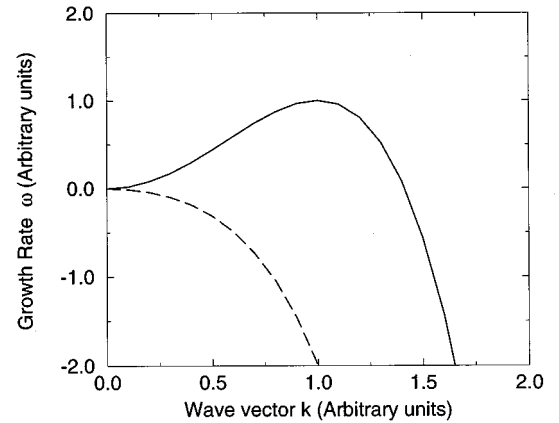
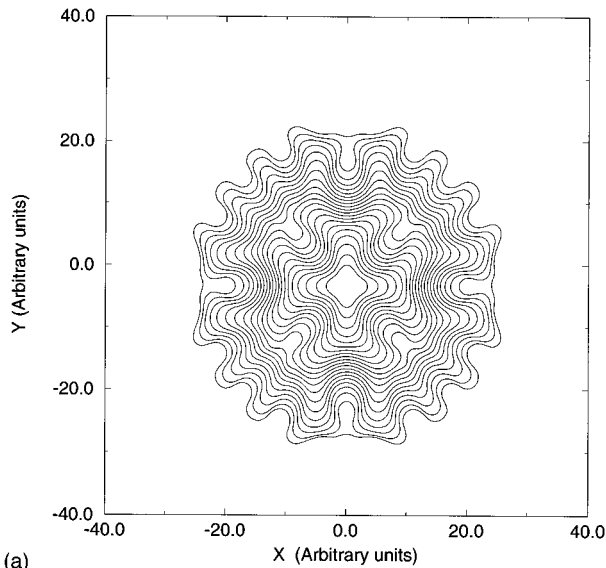
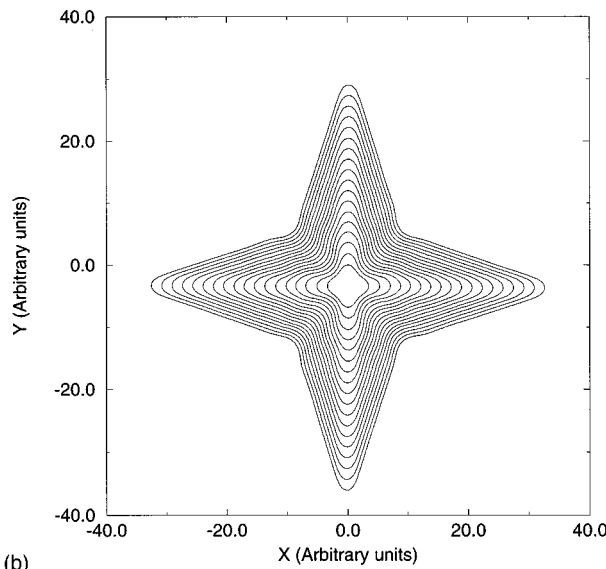


FIG. 5. The growth rate  $\omega$  as a function of the wave number. Full line: unstable. Dashed line: stable. Perturbations are analyzed as  $e^{iqx + \omega t}$ , where  $\omega$  is the growth rate and  $k$  the wave number. Wave numbers having  $\omega > 0$  ( $\omega < 0$ ) correspond to unstable (stable) modes.



(a)



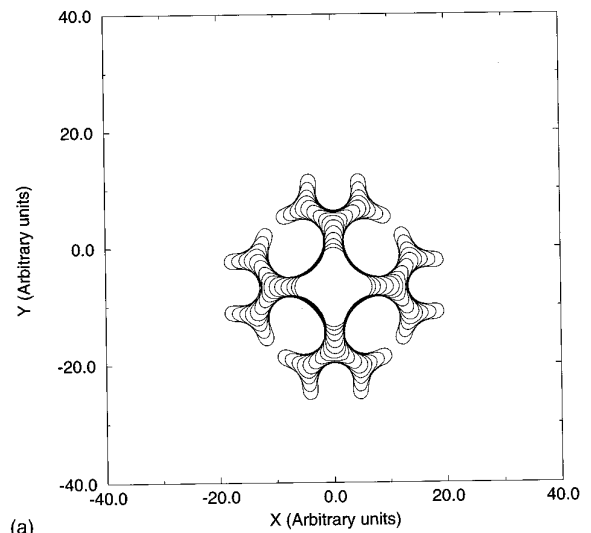
(b)

FIG. 6. A typical pattern when the constant velocity solution exists. Here Eq. (49) is solved with  $v_n$  given by Eq. (47). The parameters used are  $c=1$ ,  $a_0=a_1=a_2=1$ , and  $b_1=[1-\nu\cos(4\theta)]$ . Other choices led to the same qualitative features. (a) No crystalline anisotropy ( $\nu=0$ ), (b) with crystalline anisotropy ( $\nu=0.1$ ).

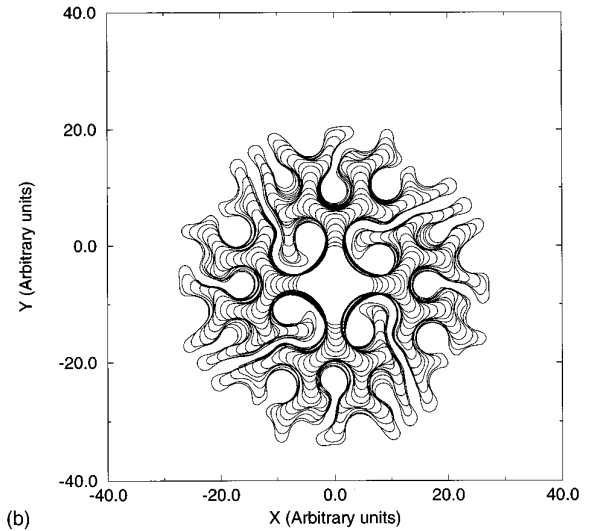
those perturbations which are likely to grow first. If the subsequent morphology is to be determined and/or the long time behavior to be ascertained, then a nonlinear analysis is necessary.

We may use a Green's function technique in order to derive a nonlinear integro-differential equation for the CP-EP boundary. This treatment will be postponed to the future. Here we shall focus on rather general nonlinear features based on symmetry arguments together with a gauge-field-invariant formulation.

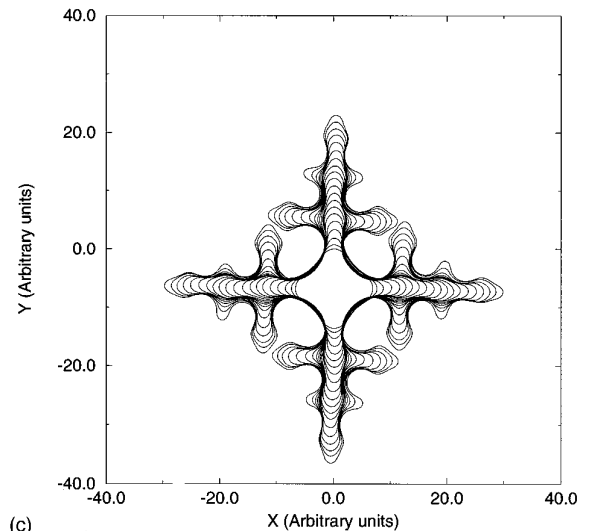
This method consists first in writing the evolution of the geometry. Because of the one dimensional character of the boundary, we shall be concerned with a string geometry. Let  $\mathbf{r}(\alpha, t)$  be the instantaneous position of the "string," where  $\alpha$  is a string parametrization which can be chosen at liberty



(a)



(b)



(c)

FIG. 7. A typical pattern in the presence of similarity solution. (a), (b) No crystalline anisotropy ( $\nu=0$ ), (c) with crystalline anisotropy ( $\nu=0.1$ ). In the simulation (b), we have implemented in our numerical code rules which mimic the repulsion. Other parameters as used in Fig. 6.

to be time independent. For a closed geometry the tangential velocity is a gauge and is fixed once the parametrization is fixed. Let  $\kappa(s,t)$  be the curvature, where  $s$  is the arclength element, and  $v_n$  the normal velocity. The curvature obeys the integral equation [13]

$$\left. \frac{\partial \kappa}{\partial t} \right|_s = - \left( \frac{\partial^2}{\partial s^2} + \kappa^2 \right) v_n - \frac{\partial \kappa}{\partial s} \int_0^s ds' \kappa v_n \quad (45)$$

and the polar angle  $\theta$  (between the normal and some axis, say  $y$ ) obeys the equation

$$\left. \frac{\partial \theta}{\partial t} \right|_s = - \frac{\partial v_n}{\partial s} - \kappa \int_0^s ds' \kappa v_n. \quad (46)$$

As in most gauge problems, a gauge-invariant formulation introduces non-locality. Note that the physics is contained in  $v_n$ .

### A. Generic limiting cases

Let us focus on the curvature evolution. The normal velocity should be invariant under reparametrization of the interface. Therefore  $v_n$  is a function of the curvature and its covariant derivatives only. The normal velocity  $v_n$  must have the following form:

$$v_n = c + a_0 \kappa + a_1 \kappa^2 + a_2 \kappa^3 + \dots + b_1 \frac{\partial^2 \kappa}{\partial s^2} + \dots \quad (47)$$

Note that the presence of the constant term  $c$  is very important. In the limit of a straight front, only  $c$  survives, and we recover our straight front solution moving at a constant speed  $c$ . For a circle  $\kappa(s,t) = \kappa(t)$  and it follows immediately from Eq. (45) that  $\kappa$  obeys  $\dot{\kappa} = -c\kappa^2$ . This equation is solved for  $R = 1/\kappa = ct$ . That is to say, a straight geometry moving at a constant speed implies that a circular geometry solution exists where the radius increases proportionally with time.

We turn now to the case of a weakly curved front. We can represent the front by its Cartesian coordinates  $h(x,t)$ , where  $s \sim x$ , and  $\kappa \sim h_{xx}$  (derivatives are subscripted). In the long wavelength limit and the slow time evolution (a situation encountered close enough to the instability threshold), it is a simple matter to show that Eq. (45) reduces to leading order to

$$h_t = -a_0 h_{xx} - b_1 h_{xxxx} + \frac{c}{2} h_x^2, \quad (48)$$

which is nothing but the Kuramoto-Sivashinsky equation, for which we have already given a universal foundation in a recent paper by using another philosophy [23]. From the linear stability analysis we have identified an instability which must be here signified by  $a_0$  being positive. For a physically well behaved system  $b_1$  must be positive in order that the fourth derivative plays the role of a short cutoff. Equation (48) is well known to produce spatiotemporal chaos. Had  $a_0$  been negative, then there would have been no need to introduce the fourth derivative (since there is no instability, and there would be no need for a cutoff). By adding a Langevin force to  $v_n$ , we would have obtained the Kardar-Parisi-

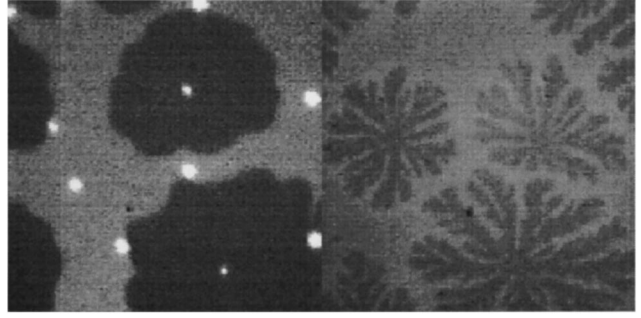


FIG. 8. Observation of the growth of two dimensional solid domains in the dodecanol monolayer [11], over a subphase containing 1.9 nM octanoid acid. Left panel:  $pH=12$  adjusted by NaOH. In this case impurities are miscible in water; right panel:  $pH=2$  adjusted by HCl addition. Here impurities are not miscible in water.

Zhang equation [24], which has been widely used as an attempt to describe kinetic roughening during molecular beam epitaxy.

### B. Strongly curved fronts

For a more curved front we have analyzed the equation numerically. We have used a parametrization of the front so that the relative arclength  $s/L$  remains constant, where  $L$  is the total length for the closed geometry. In such reparametrization, it can be shown that  $\kappa$  obeys the equation

$$\frac{\partial \kappa}{\partial t} = - \left( \frac{\partial^2}{\partial s^2} + \kappa^2 \right) v_n + \frac{\partial \kappa}{\partial s} \left( \frac{s}{L} \oint ds' \kappa v_n - \int_0^s ds' \kappa v_n \right), \quad (49)$$

and where the total length is governed by

$$\frac{\partial L}{\partial t} = \oint ds' \kappa v_n. \quad (50)$$

Numerical results [using Eq. (48)] reveals that the presence of the constant term  $c$  (which follows from the existence of the straight front solution) leads to compact patterns as shown in Fig. 6, while in its absence patterns like those shown in Fig. 7 are expected. We note that in Fig. 7, a ‘‘cascade’’ of tip splitting occurs and leads to a strongly branched structure. Here since our model is local, it does not prevent crossing, as expected from repulsion via a diffusion field. By implementing rules in our code which mimic this repulsion, we confirm the above assertion about the ‘‘tip-splitting cascade’’ [see Fig. 7(b)]. We plan to give a detailed description of our finding in the future. Note finally that the patterns shown in Figs. 6(a) and 7(a) bear a quite good resemblance to experimental observations of Lenne *et al.* (see Fig. 8).

## VII. CONCLUSION

We have developed a physical description of growth of a condensed phase at the expense of the expanded one where impurities are miscible in water. We have shown that diffusion in the bulk completely destroys the similarity solution. A straight front solution becomes possible. This is attributed to a dimensional reason: bulk diffusion brings out a new length scale. We have provided an analytical solution for the

straight front and have analyzed its stability. We have argued physically that the existence of a straight front solution should lead generically to a compact pattern. Our nonlinear analysis has confirmed our expectation. In this first paper we have focused on general features with regard to nonlinear development. That is, we have used a geometrical representation of the “string” combined with symmetries. We have shown that for a weakly curved front, dynamics fall onto a universal Kuramoto-Sivashinsky one, which generates weak “turbulence.” For a strongly curved front compact patterns are exhibited both with and without crystalline anisotropy.

The Langmuir systems are rather unique in that the boundary between the condensed phase and the expanded one is truly one dimensional. In principle, we should expect the boundary to be rough at all temperatures. In other words,

statistical fluctuations must come to the fore and should strongly compete with the deterministic instability studied here. It seems a bit premature on the experimental level to impose an initial straight front which undergoes a morphological instability at a critical speed, and thereby to study in a controlled way competition between noise and determinism. We are, however, confident that this should open new and decisive lines of inquiries in the near future.

#### ACKNOWLEDGMENTS

We benefited from several valuable discussions with B. Berge and P.F. Lenne. We are grateful to the “Centre Grenoble de Calcul Vectoriel” for providing us with computing facilities. We thank S. Akamatsu for Fig. 3.

- 
- [1] A. Pockels, *Nature (London)* **43**, 437 (1891).
  - [2] H. Mohwald, *Annu. Rev. A* **41**, 441 (1990).
  - [3] J. Prost and F. Rondelez, *Supplement to Nature (London)* **350**, 6319 (1990).
  - [4] D. Andelman, F. Brochard, and J.F. Joanny, *J. Chem. Phys.* **86**, 3673 (1986).
  - [5] S. Akamatsu and F. Rondelez, *J. Phys. (France) II* **1**, 1309 (1991).
  - [6] S. Akamatsu, O. Bouloussa, K. To, and F. Rondelez, *Phys. Rev. A* **46**, R4504 (1992).
  - [7] B. Berge, O. Okonov, J. Lajzerowicz, A. Renault, J.P. Rieu, M. Vallade, J. Als-Nielsen, G. Grubel, and J.F. Legrand, *Phys. Rev. Lett.* **73**, 1652 (1994).
  - [8] K. Stine, S.A. Raueo, B.G. Moore, J.A. Wise, and C.M. Knobler, *Phys. Rev. A* **41**, 6884 (1990).
  - [9] B.I. Halperin and D.R. Nelson, *Phys. Rev. Lett.* **41**, 121 (1978).
  - [10] F. Bonosi, A. Renault, and B. Berge (unpublished).
  - [11] P.F. Lenne, A. Valance, F. Bonosi, C. Misbah, and B. Berge (unpublished).
  - [12] B. Berge and P.F. Lenne (unpublished).
  - [13] D. Kessler, J. Koplik, and H. Levine, *Adv. Phys.* **37**, 255 (1988).
  - [14] J.S. Langer, in *Chance and Matter*, edited by J. Souletie (North-Holland, Amsterdam, 1987).
  - [15] G.P. Ivantsov, *Dokl. Akad. Nauk SSSR* **58**, 567 (1947).
  - [16] E. Brener, H. Müller-Krumbhaar, and D.E. Temkin, *Europhys. Lett.* **17**, 535 (1992); T. Ihle and H. Müller-Krumbhaar, *Phys. Rev. E* **49**, 2972 (1994).
  - [17] Y. Kuramoto, *Suppl. Prog. Theor. Phys.* **64**, 346 (1978); G.I. Sivashinsky, *Acta Astronaut.* **4**, 1177 (1977).
  - [18] I. Bena, C. Misbah, and A. Valance, *Phys. Rev. B* **47**, 7408 (1993).
  - [19] J.S. Langer, *Rev. Mod. Phys.* **52**, 1 (1980).
  - [20] P. Pelcé and Y. Pomeau, *Stud. Appl. Math.* **74**, 245 (1986).
  - [21] M. Uwaha and Y. Saito, *Phys. Rev. A* **40**, 4716 (1989).
  - [22] Using the propagator formalism and starting from arbitrary initial conditions, one can show that at short time (in comparison with  $\tau$ ) the behavior is fixed by the similarity solution. At later time the solution tends to the constant speed one.
  - [23] C. Misbah and A. Valance, *Phys. Rev. E* **49**, 166 (1994).
  - [24] M. Kardar, G. Parisi, and Y. Zhang, *Phys. Rev. Lett.* **56**, 889 (1986).